Research in Pharmaceutical Sciences, August 2024; 19(4): 397-414
Received: 04-04-2024
Peer Reviewed: 28-04-2024
Revised: 14-06-2024
Accepted: 27-07-2024
Published: 16-08-2024

School of Pharmacy & Pharmaceutical Sciences
Isfahan University of Medical Sciences

Original Article

Oral administration of crocin-loaded solid lipid nanoparticles inhibits neuroinflammation in a rat model of epileptic seizures by activating SIRT1 expression

Seyran Kakebaraei[1,2], Mohammadreza Gholami[1], Touraj Zamir Nasta[3], Elham Arkan[4], Fariborz Bahrehmand[3], Sajad Fakhri[5], and Cyrus Jalili[3,*]

[1]*Department of Anatomical Sciences, Kermanshah University of Medical Sciences, Kermanshah, Iran.*
[2]*Students Research Committee, Kermanshah University of Medical Sciences, Kermanshah, Iran.*
[3]*Medical Biology Research Center, Health Technology Institute, Kermanshah University of Medical Sciences, Kermanshah, Iran.*
[4]*Nano Drug Delivery Research Center, Health Technology Institute, Kermanshah University of Medical Sciences, Kermanshah, Iran.*
[5]*Pharmaceutical Sciences Research Center, Health Institute, Kermanshah University of Medical Sciences, Kermanshah, Iran.*

Abstract

Background and purpose: Epilepsy is a group of chronic neurological diseases caused by a complex set of neuronal hyper electrical activities and oxidative stress of neurons. Crocin is a natural bioactive agent of saffron with different pharmacological properties and low bioavailability. This study aimed to evaluate crocin-loaded solid lipid nanoparticles (SLNC) for neuroprotection activity and efficacy against pentylenetetrazol (PTZ)-induced epilepsy.

Experimental approach: The rats were pretreated with SLNC and pure-crocin (PC; 25 and 50 mg/kg/day; P.O.) for 28 days before PTZ induction. Behavioral functions were evaluated by passive avoidance learning (PAL) tasks. Then, total antioxidant capacity (TAC), malondialdehyde (MDA), and pro-inflammatory factors were measured in the brain tissue using ELISA kits. Gene expression levels were analyzed with real-time polymerase chain reaction and immunohistochemical assay was used to assess the protein expression of sirtuin1 SIRT 1).

Findings/Results: SLNC was prepared with an average particle size of 98.25 nm and 98.33% encapsulation efficiency. Memory deficit improved in rats treated with SLNC. Administering SLNC at 25 and 50 mg/kg significantly reduced MDA and proinflammatory cytokines while increasing TAC. Additionally, administering SLNC before treatment increased the levels of SIRT1, peroxisome proliferator-activated receptor coactivator 1α, cAMP-regulated enhancer binding protein, and brain-derived neurotrophic factor. Furthermore, SLNC administration resulted in the downregulation of caspase-3 and inflammation factor expression.

Conclusion and implications: Overall, the obtained results showed that SLNC has better protective effects on oxidative stress in neurons, neurocognitive function, and anti-apoptotic and neuromodulatory activity than PC, suggesting that it is a promising therapeutic strategy for inhibiting seizures.

Keywords: Crocin; Epilepsy; Neuroinflammation; PGC-1α; SIRT1; Solid lipid nanoparticles.

INTRODUCTION

The mitochondrion is an organelle critical for energy supply and a site for the production of reactive oxygen species (ROS) and their accumulation. It plays an affirmative role in the development of neurodegenerative disorders, including epilepsy (1,2). Epilepsy is a devastating disturbance of the central nervous system (CNS) that involves an uncontrollable electrical discharge from a group of neurons, accompanied by recurrent, unexcitable seizures. Epileptic attacks can be tied to damage to the cerebrovascular system, brain damage, inflammation, tumors, and hypoxia (3,4).

*Corresponding author: C. Jalili
Tel: +98-9188317220, Fax: +98-8334274622
Email: cjalili@kums.ac.ir, cjalili@yahoo.com

Access this article online	
	Website: http://rps.mui.ac.ir
	DOI: 10.4103/RPS.RPS_68_24

Peroxisome proliferator-activated receptor coactivator 1α (PGC-1α) signaling pathway is a significant modulator of glucose homeostasis, lipid catabolism, and mitochondrial biogenesis, enhancing mitochondrial efficacy and intracellular ATP production. The upregulation of ROS of detoxification enzymes reduces the oxidative stress that induces epilepsy (1,5). Mammals have seven sirtuins (sirt1-7). Sirtuin is NAD^+-dependent deacetylases, which show principal roles in responding to neuronal degeneration pathways by regulating axonogenesis, neuron outgrowth, and neuron survival (6). Oxidative stress creates a disturbance in the overgeneration and agglomeration of ROS, combined with the diminution of the antioxidant action, highlighting notable signs of epileptogenesis (7). Seizures are accompanied by the overexpression of proinflammatory cytokines, including interleukin-1 beta (IL-1β), tumor necrosis factor-alpha (TNF-α), nuclear factor kappa B (NF-κB), and nitric oxide synthase (iNOS), which eventually leads to neuronal hyperexcitability and cell death (8,9). Saffron (*Crocus sativus* L.) has broadly been used as a condiment, food coloring, and for herbal medicine aims in the Mediterranean region for centuries. Its protective effects result from its effective ingredients, *e.g.* crocin and crocetin. Crocin, a high water solubility carotenoid-rich, is saffron's most hallmark and plentiful antioxidant compound (10). Studies have proven that crocin possesses different pharmacological properties such as anti-inflammatory, anti-tumor, antioxidant, antianxiety and hypnotic, and antidepressant effects, improves neurological disorders and cognition, and enhances learning capability (10-13). On the other hand, another study showed that crocin is effectless on PTZ-induced clonic seizures (14). Due to this contradiction, further investigation to evaluate the antiepileptic effects of crocin in animal models is required. Advancement and biological properties of nanotechnology-based drug delivery have led to the progression of solid lipid nanoparticles (SLN), liposomes, nanoencapsulation, and micelles that have lately been used for transferring therapeutic agents in diverse CNS-related diseases (15). SLNs are proper nanocarrier systems for the distribution of hydrophobic and lipophilic combinations. SLNs are a novel prototype of nano/submicron-sized particles (50-1000 nm) where an illiquid lipid has interchanged with the fluid lipid (oil) (16,17). SLNs have emerged as a new type of carrier system in recent years. They offer an alternative to traditional carriers like emulsions, liposomes, and polymeric nanoparticles. Unlike these older carriers, SLNs use solid lipids instead of liquid lipids. This shift has resulted in submicron-sized lipid emulsions that possess several advantages. SLNs have small particle sizes, providing a large surface area for interactions. They also have a high capacity for drug loading and offer interfacial phase interactions. These characteristics make SLNs an attractive option for improving the effectiveness of pharmaceuticals, nutraceuticals, and other materials (18). Encapsulating crocin in SLNs can enhance its ability to cross the brain. Furthermore, this approach may help address its rapid metabolism and low bioavailability.

This is the first time the antiepileptic effects of crocin-loaded SLNs (SLNC) have been examined on memory and inflammatory profiles. Previous studies have shown that crocetin, a related compound, can cross the blood-brain barrier (BBB) (19). However, no concrete evidence has confirmed whether this bioactive compound can behave similarly. Nano-antioxidants can create an emerging strategy in passing antioxidants to enhance the potential of neurologic disorders' prevention and therapy due to oxidative damage (20). Therefore, this study investigates the improvement to the neuroprotective role of SLNC against PTZ-induced acute epileptic seizures in the adult rat model, overcoming the problems of low solubility of PC, protecting it from the destructive effect of GI tract and improving delivery of active substance by crossing the blood-brain barrier (BBB) to enhance the SIRT1, PGC-1α, brain-derived neurotrophic factor (BDNF), and cAMP-regulated enhancer binding protein (CREB-1) expression in the hippocampus area, and to decrease the oxidation, apoptosis (caspase3), and inflammation markers.

MATERIALS AND METHODS

Chemicals

Crocin (purity ≥ 98%), PTZ, stearic acid, lecithin, chloroform, polysorbate 80 (Tween® 80), a dialysis bag (molecular weight cut off of 12 KD), ethylenediaminetetraacetic acid (EDTA), and ethanol are purchased from Sigma-Aldrich (Germany). The anti-sirt1 antibody (Cat. No. ab110304) is obtained from Abcam (Cambridge, UK). All chemicals or solvents used in the research were of analytical grade.

Preparation of SLN and SLNC

The fabrication of SLNC was freshly performed in pure water. Briefly, stearic acid (10 mM) was dissolved at 75 °C in pure water (lipid phase), and then crocin (3 g), lecithin (10 mM), and Tween® 80 were dissolved in 10 mL pure water (the aqueous phase). After the lipid phase was dissolved, The aqueous phase was then added to the lipid phase stirring on a magnet stirrer for 25 min. Afterward, the final dispersion was homogenized on ice for 15 min at 80 W using an ultrasonic homogenizer (Fanbolun Company, China). The supernatant of the final mixture was analyzed by a UV-VIS spectrophotometer at 470 nm. Plain SLN (blank) was manufactured using the same method without incorporating the crocin (21).

Physicochemical characterization of SLNC

Particle size, polydispersity index, and zeta potential

The polydispersity index (PDI), particle average (Z-average), and zeta potential of the nanoparticles (SLNC) in suspension were assessed by Zetasizer (Malvern, Worcestershire, UK) using a dynamic light scattering (DLS) mode at 25 °C. The evaluations were reduplicated thrice for each sample.

Drug loading content and entrapment efficiency

The amount of crocin loaded into SLNCs was assessed as follows: the mixture (SLNC) was centrifuged (rpm, 30 min), and the supernatant containing the free crocin (un-entrapped in nanoparticles) was evaluated for free crocin measurements using a UV-VIS spectrophotometer (Philips PU 8620, USA) at 470 nm. The entrapment efficiency (EE%; Eq. 1) and the drug loading percent (DL%; Eq. 2) were computed using the following equations (22):

$$EE\ (\%) = \frac{Total\ drug - free\ drug}{Total\ drug} \times 100 \quad (1)$$

$$DL\ (\%) = \frac{Total\ drug - free\ drug}{Total\ weight\ of\ nanoparticles} \times 100 \quad (2)$$

Transmission electron microscopy

The morphological characterization of SLNC was examined using transmission electron microscopy (TEM) for aggregation and uniformity in size and shape. In summary, SLNC was spread onto the copper grid and observed under TEM (Zeiss, Sigma VP, Germany). Photo-micrographs of SLNC were taken at an appropriate magnification.

Field emission scanning electron microscopy

The surface and shape of SLNC were visualized using field-emission scanning electron microscopy (FE-SEM; Zeiss, Sigma VP, Germany). The SLNC was covered with gold using an ion sputter. Photo-micrographs of SLNC are taken at an appropriate magnification.

Fourier transform infrared spectroscopy

The pure crocin, SLNC, and SLN were analyzed using a Fourier transform infrared spectroscopy (FT-IR; Shimadzu Co., Japan) to determine the intermolecular interaction of various functional groups (potassium bromide method). The spectra of crocin, SLN, and SLNC were measured over the scanning range of 200-4000 cm^{-1}.

In vitro release study

In vitro release patterns of the drug from nanoparticles (SLNC) were examined as follows: Briefly, the SLNC was diffused in 80 mL of phosphate-buffered saline (PBS; pH 7.4) in dialysis bags, under stirring for 72 h at 37 ± 0.5 ℃. At appropriate time intervals (0, 0.5, 1, 2, 3, 4, 5, 6, 12, 24, 48, and 72 h), one mL of the release medium was removed and replaced with an equal volume of fresh PBS. The concentration of crocin released from the nanoparticles was measured by a UV-VIS spectrophotometer set at 470 nm.

Calculation of lethal dose of SLNC

The median lethal dose (LD_{50}) of SLNC was determined using the oral procedure on Wistar rats according to the Reed and Muench method (23).

Animals and treatment schedule

Fifty-six male Wistar rats weighing 180-200 g were procured from the Pasteur Institute of Iran, Tehran. The rats were acclimatized for seven days before starting the study. All the experimental protocols used in the study were confirmed by the Ethics Committee of the Kermanshah University of Medical Sciences, Kermanshah, Iran (Ethic No. IR.KUMS.AEC.1401.008). The animals were distributed into seven groups of 8 each (Table 1). Rats (except the naïve control group (I) and PTZ-group (II) that orally received 0.9% NaCl) were given PC and SLNC orally at 25 and 50 mg/kg once a day for 28 days. After 4 weeks of SLNC or saline administration, epileptic seizures were induced by intraperitoneal injection of a single dose of PTZ at 75 mg/kg. Based on a previous study, the seizure severity was scored as follows (24). 0, no change in behavior; 1, contraction of the face and hands' muscles; 2, diffusion of contractile wave around the body; 3, myoclonic jerks and standing on two feet; 4, tonic-clonic attacks and falling on the side; 5, tonic-clonic attacks and falling on the back. Animals that reached phases 4/5 were included in the experiment.

Passive avoidance learning and memory

Passive avoidance learning (PAL) was assessed using a shuttle box. This device is made of two black and white chambers of the same size (22 × 22 × 32 cm). The two chambers are separated by a barrier. The floor of the two rooms is worn by steel rods (0.5 cm diameter) spaced 1 cm independently. At the bottom of the black chamber, there is an electrifying grid floor (50 Hz, 3 s), with an intensity of 0.7 mA. At this stage (24 h after the last training phase), the retention test was assessed. Each rat was sustained in the white chamber for 10 s, and then the barrier was raised. The latency time of the rat to enter the black box (step-through latency (STL)) was registered. The retention phase followed for 600 s. In this course, no electric shock was delivered.

Estimation of inflammatory cytokines

Determination of proinflammatory factors IL-1β, TNF-α, and NF-κB in brain tissue was evaluated using the required ELISA kits (Fivephoton Biochemicals, CA 92117, USA).

Total antioxidant capacity

To evaluate total antioxidant capacity (TAC), the brain tissue was homogenized in PBS (pH 7.0) and centrifuged, and then the supernatant was frozen at -80 °C. Ferric reducing antioxidant power (FRAP) was made by a combination of 300 mmol/L acetate buffer with 10 mM 4,6-tripyridyl-S-triazine (TPTZ) in HCl and $FeCl_3$. Then, the FRAP reagent was added to the samples and incubated. The absorbance was measured at 593 nm using a spectrophotometer.

Lipid peroxidation assay

Tissue brain homogenization was used to assess malondialdehyde (MDA) levels in PBS solution (pH 7.4). The homogenized tissues were centrifuged at 3000 rpm for 15 min. Accordingly, thiobarbituric acid reactive substances (TBARS; 5.2 mg/mL) were added to the supernatant and incubated at 95 °C for 45 min and centrifuged again at 3000 rpm. The absorbance was recorded at 532 nm.

Table 1. Treatment schedule for different experimental groups.

Number	Groups	Treatment (PO/IP, rat)
I	Naïve control	0.9% NaCl for 4 weeks
II[b]	PTZ	0.9% NaCl + PTZ (75 mg/kg)
III[a]	SLNC 25 + PTZ	SLNC (25 mg/kg/day) + PTZ (75 mg/kg)
IV[a]	SLNC 50 + PTZ	SLNC (50 mg/kg/day) + PTZ (75 mg/kg)
V[a]	PC 25 + PTZ	PC (25 mg/kg/day) + PTZ (75 mg/kg)
VI[a]	PC 50 + PTZ	PC (50 mg/kg/day) + PTZ (75 mg/kg)
VII[a]	Blank-SLN + PTZ	Blank-SLN + PTZ (75 mg/kg)

a, Groups III-VII received SLNC, PC and blank-SLN for 4 weeks through oral gavage, and then on day 28, the rats were administrated a single dose of PTZ (75 mg/kg); b, group II received 0.9% NaCl for 4 weeks and on day 28, the rats were administrated a single dose of PTZ (75 mg/kg); SLNC, crocin-loaded solid lipid nanoparticle; PTZ, pentylenetetrazol; PC, pure crocin.

Table 2. Sequence of the primers used for real-time polymerase chain reaction analysis.

Gene name	Primer's sequence	Size
GAPDH	Forward: AGTTCAACGGCACAGTCAAG Reverse: TACTCAGCACCAGCATCACC	119
PGC-1α	Forward: GCAACATGCTCAAGCCAAAC Reverse: TGCAGTTCCAGAGAGTTCCA	133
Sirt1	Forward: CCAGAACAGTTTCATAGAGCCA Reverse: CACTTCATGGGGTATAGAACTTGG	126
BDNF	Forward: TGCTTTGGGGCAGACGA Reverse: ACCTGGTGGAACTCAGGG	126
CREB-1	Forward: CGAGAACCAGCAGAGTGGAG Reverse: TTCACTGACATCCTGCTTTACAAT	135
TNF-α	Forward: GTCTTCTGCCTGCTGCACTTTG Reverse: ATGGGCTACAGGCTTGTCACTC	186
IL-1β	Forward: CAGAGCCACATGCTCCTAGA Reverse: TGTCCAGCTGGTCCTTTGTT	118
Caspase-3	Forward: GCAGCAGCCTCAAATTGTTGAC Reverse: TGCTCCGGCTCAAACCATC	144

PGC-1α, proliferator-activated receptor coactivator 1α; Sirt, sirtuins; BDNF, brain-derived neurotrophic factor; CREB-1, cAMP-regulated enhancer binding protein; TNF-α, tumor necrosis factor-alpha; IL-1β, interleukin-1 beta.

Real-time polymerase chain reaction

To evaluate the effect SLNC and PC on the expression of BDNF, CREB-1, SIRT1, PGC-1α, caspase-3, TNF-α, and IL-1β, the mRNA in the rat's hippocampal tissue was isolated using TRIZOL and chloroform methods, and then the purity of mRNA samples was determined by Nanodrop (ThermoFisher Scientific, USA). Complementary DNA (cDNA) was synthesized using a reverse transcriptase kit (Takara, Japan). Quantitative real-time polymerase chain reaction (qPCR) was carried out using Stem Gene Realtime SYBR Green 2x Master (Takara, Japan) on RunMei Q200. The forward and reverse primer sequences are shown in Table 2. mRNA expression was assessed as the relative fold changes according to the $2^{-\Delta\Delta Ct}$ formula.

Immunohistochemical examinations

The hippocampal tissue sections were incubated for 25 min at 60 °C and then deparaffinized and rehydrated. The tissues are immersed in sodium citrate buffer staining, which was performed according to the manufacturer's protocol (Abcam, USA) and the previously reported method (25). The tissue sections were covered with dH_2O and incubated with peroxidase blocking reagent (0.03%) for 1 h. The slides were coated with the anti-sirt1 primary antibodies (2 h at 4 °C) and then incubated with streptavidin conjugated to horseradish peroxidase and 3,3′-diaminobenzidine (DAB) for 10 min. The tissue sections are counterstained with hematoxylin. Scoring of immunohistochemically-stained neurocytes was done under light microscopy. The SIRT1-positive cells were counted in 5 fields of the hippocampal tissue randomly, at 400 × magnification. Finally, the software calculated the cellular distribution.

Statistical analyses

The data are expressed as mean ± SEM. One-way analysis of variance (ANOVA) followed by Tukey post-hoc test was employed to analyze the parametric data using GraphPad Prism software 9.5.1 (LaJolla, USA). Data from the PAL method was assessed using the Kruskal-Wallis nonparametric test followed by Dunn's test. The *P*-values < 0.05 were considered statistically significant.

RESULTS

Physiochemical properties of SLNs and SLNC

The physicochemical properties of plain and crocin-loaded SLNs are shown in Table 3.

Table 3. Physicochemical features of the different nanoparticles. Data are presented as mean ± SD. The experiment is repeated three times.

Particles	Z-average diameter (nm)	Polydispersity	Zeta potential (mV)	Entrapment efficiency (%)	Drug loading (%)
Blank-SLN	66.2 ± 1.5	0.17 ± 0.047	-22.03 ± 6.43	---	---
SLNC	98.25 ± 0.5	0.11 ± 0.13	-33.45 ± 8.15	98.33	26.8

SLNC, crocin-loaded solid lipid nanoparticle

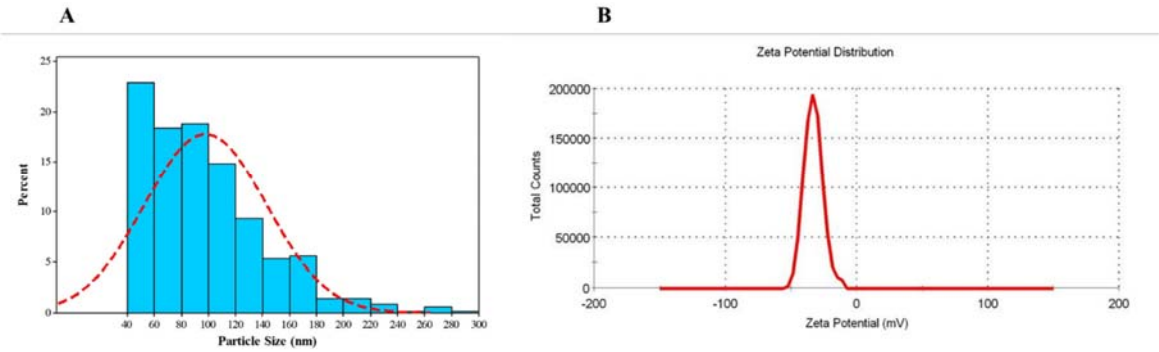

Fig. 1. Physicochemical characterization of SLNC by Zetasizer instrument: (A) the particle size and (B) zeta potential. SLNC, Crocin-loaded solid lipid nanoparticle.

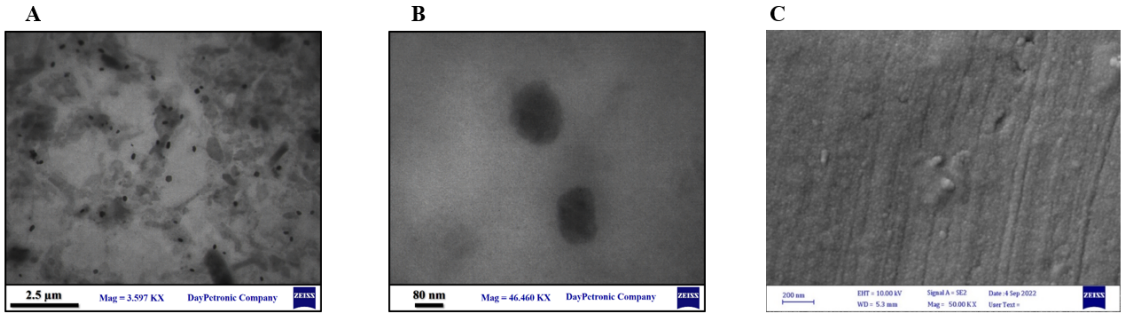

Fig. 2. (A and B) Transmission electron microscopy and (C) field emission scanning electron microscopy analysis of the optimized SLNC. SLNC is presented with red arrows. SLNC, Crocin-loaded solid lipid nanoparticle.

The average particle size and zeta potential of the SLNC were approximately 98.25 nm and -33.45 mV, respectively (Fig. 1A and B). For all formulations, the PDI was less than 0.2. The shape and morphology examination of the SLNC with a regular spherical construction was revealed by TEM and FE-SEM (Fig. 2A-C). The DL% and EE% in SLNC formulations were 26.8% and 98.33%, respectively (Table 3)

FT-IR analysis

As shown in Fig. 3, the FT-IR spectrum of the prepared SLN indicated the characteristic peaks for N-H symmetric stretch in the lecithin at 3381 cm^{-1}. The SLN spectra also showed peaks at 1734 cm^{-1} representing C=O of the ester compound in lecithin and 2918 and 2852 cm^{-1} indicating the stretching of the C-H groups. The SLN spectra had various specific peaks analogous to the lecithin spectra without variation, but the intensity of the peaks related to lecithin was significantly reduced when they were inserted into SLN. This feature may be due to the shielding efficacy of the surfactant and its hydrophilic environment. Six characterization peaks were seen in the FT-IR spectrum of PC: sharp bands at 3427, 2922, 1492, 1193, 1118, 1041, and 684 cm^{-1} and a

broad band at 400-3900 cm^{-1}. FT-IR spectra of PC also showed bands at 1635 cm^{-1} due to the C=C bond, 1492 cm^{-1} corresponding to the C=O bond, and 2922 cm^{-1} related to the C-H bond. The peaks at 1492 cm^{-1} and 1041 cm^{-1} could be attributed to the stretching oscillations of C=O in the carbonyl group and the C-O stretching vibration, respectively, which can be related to the sugar functional groups in crocin structures (Fig. 3). The broad stretch 3427 and 3419 cm^{-1} correspond to the presence of group OH. FT-IR spectrum of crocin-coated SLN showed the unique bands of OH at 3427 and 3419 cm^{-1}, which were present only in crocin. This confirms the successful interaction of SLN with crocin indicating the strong hydrophobicity character of the samples. Thus, the characteristic peaks between SLN and SLNC could be due to the hydrogen bond constitution when crocin is implanted into SLN (21,26).

The in vitro release

According to our results, the SLNC formulation showed sustained release behavior with an accumulative percent of crocin release (SLNC) of about 29% of the drug over 10 h. Then, about 40% after 24 h, and eventually 45% of the crocin was released from the nanoparticles after 48 h (Fig. 4).

LD_{50} of SLNC

From the results of LD_{50}, the content of the tested SLNC was found to be 25 and 50 mg/kg of the drug after oral administration. These doses did not cause any adverse effects.

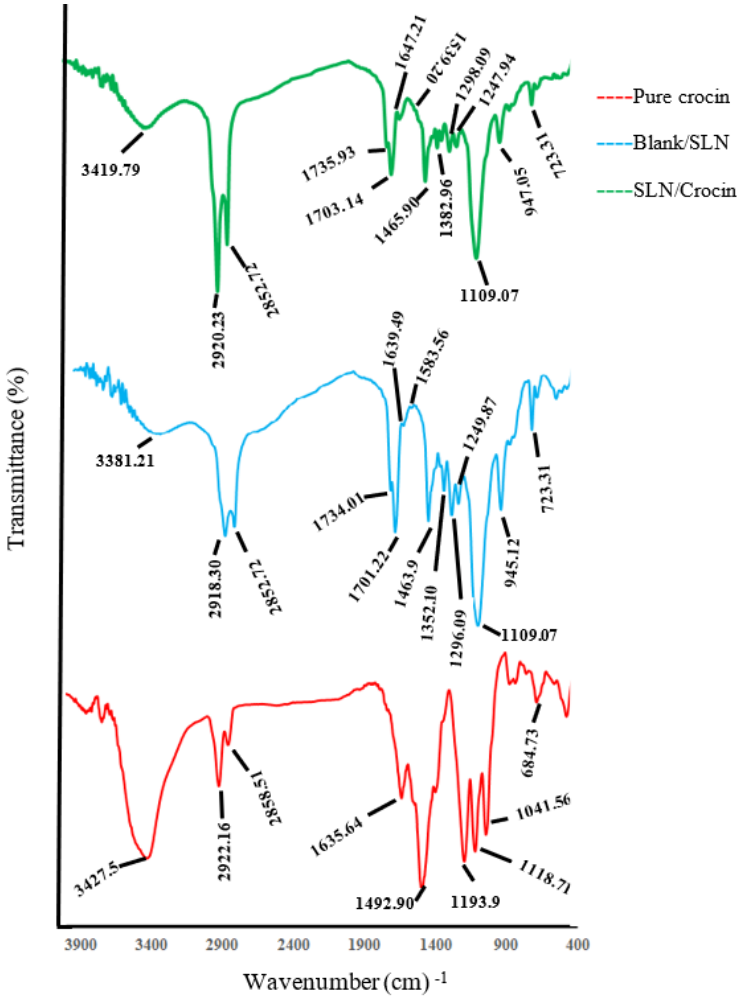

Fig. 3. Fourier-transform infrared spectroscopy diagrams of the single pure crocin, blank, and SLNC. SLNC, Crocin-loaded solid lipid nanoparticle.

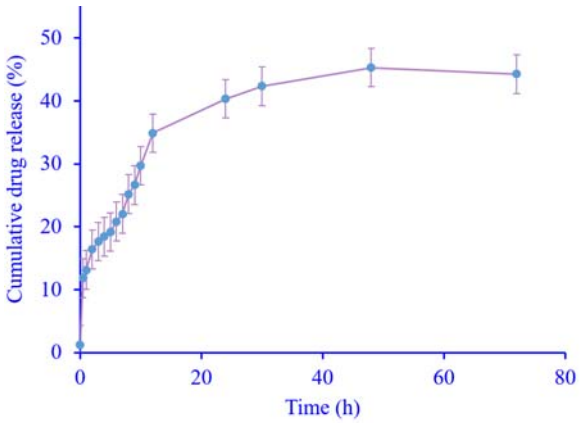

Fig. 4. *In vitro* drug release profiles of crocin from single SLNC and with the dialysis bag system in the PBS medium pH 7.4 at 37 ℃ after 72 h. SLNC, Crocin-loaded solid lipid nanoparticle.

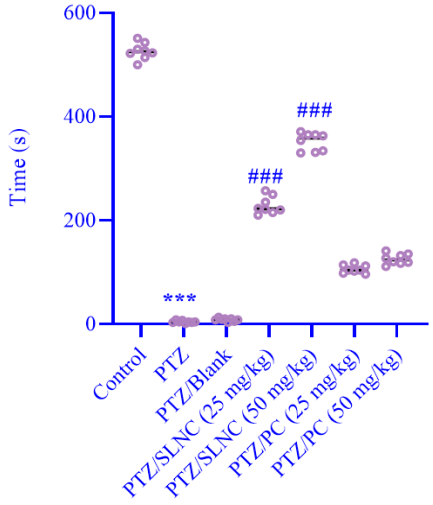

Fig. 5. Comparison of the mean step-through latency in the performance of the passive avoidance learning task in different experimental groups. Values are expressed as mean ± SEM. ***$P < 0.001$ indicates significant difference compared to the control group; $^{###}P < 0.001$ versus the PTZ-treated group. SLNC, Crocin-loaded solid lipid nanoparticle; PTZ, pentylenetetrazol; PC, pure crocin.

Effects of SLNC and PC on the acquisition of PAL

The effect of SLNC and PC on the acquisition of PAL was analyzed using the Kruskal-Wallis statistical test. According to Fig. 5, STL values were significantly reduced in the PTZ group compared to the control group. In addition, STL values in the groups treated with PTZ + SLNC (25 and 50 mg/kg) exhibited a significant increase compared to the PTZ group.

Anti-inflammatory effects of SLNC and PC following PTZ injection

The levels of NF-κB, TNF-α, and IL-1β estimate the anti-inflammatory efficacies related to SLNC and PC administration in response to PTZ-induced neuroinflammation. The PTZ group demonstrated a remarkable elevation of all assessed pro-inflammatory biomarkers including NF-κB, TNF-α, and IL-1β in brain tissues compared to the control group. In contrast, the PTZ + SLNC (25 and 50 mg/kg) pretreated groups displayed significantly decreased levels of NF-κB, TNF-α, and IL-1β in the brain tissue compared to PTZ-mediated neuronal inflammation. There were no significant differences between the PTZ + PC (25, 50 mg/kg) groups compared to the PTZ group (Fig. 6).

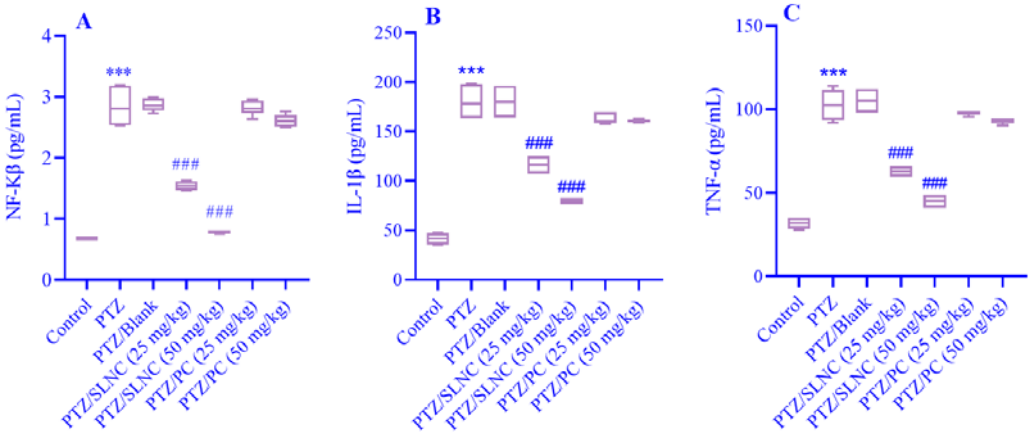

Fig. 6. Effects of orally administered SLNC and PC on the levels of inflammatory mediators (A) NF-κB, (B) IL-1β, and (C) TNF-α in brain tissue following PTZ-induced epileptic seizures. Values are expressed as mean ± SEM. ***$P < 0.001$ indicates significant difference compared to the control group; ###$P < 0.001$ versus the PTZ-treated group. SLNC, Crocin-loaded solid lipid nanoparticle; PTZ, pentylenetetrazol; PC, pure crocin; IL-1β, interleukin-1 beta; TNF-α, tumor necrosis factor-alpha; NF-κB, nuclear factor kappa B.

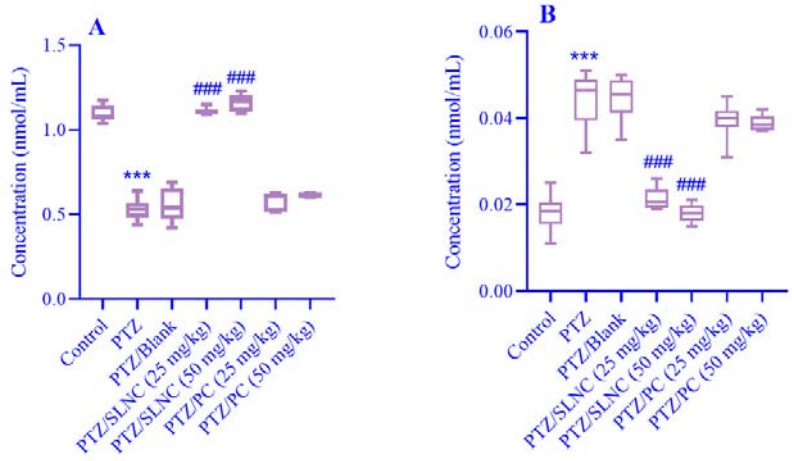

Fig. 7. Effect of the orally administered SLNC and PC on (A) total antioxidant capacity and (B) malondialdehyde. Values are expressed as mean ± SEM. ***$P < 0.001$ indicates significant difference compared to the control group; ###$P < 0.001$ versus the PTZ-treated group. SLNC, Crocin-loaded solid lipid nanoparticle; PTZ, pentylenetetrazol; PC, pure crocin.

Effect of SLNC and PC treatment on TAC and MDA levels in the brain tissue

The present data disclosed a statistically significant reduction in the TAC in the brain tissue of rats treated with PTZ compared to the control group. In addition, a significant elevation was found in the PTZ + SLNC (50 and 25 mg/kg) compared to the PTZ group (Fig. 7A). MDA level increased in the PTZ group compared to the control group. A significant decrease was observed in MDA levels of the PTZ + SLNC (50, 25 mg/kg) compared to the PTZ group (Fig. 7B). There is no meaningful difference between the PTZ + PC (25 and 50 mg/kg) groups compared to the PTZ group.

The effect of SLNC and PC treatment on the expression of BDNF and CREB-1

The mRNA expression of the BDNF and CREB-1 receptors in hippocampal tissue significantly decreased in rats receiving PTZ compared to the control group. The expression of BDNF and CREB-1 had a meaningful increase in the groups that received PTZ + SLNC (25 and 50 mg/kg) in comparison with the PTZ group (Fig. 8A and B).

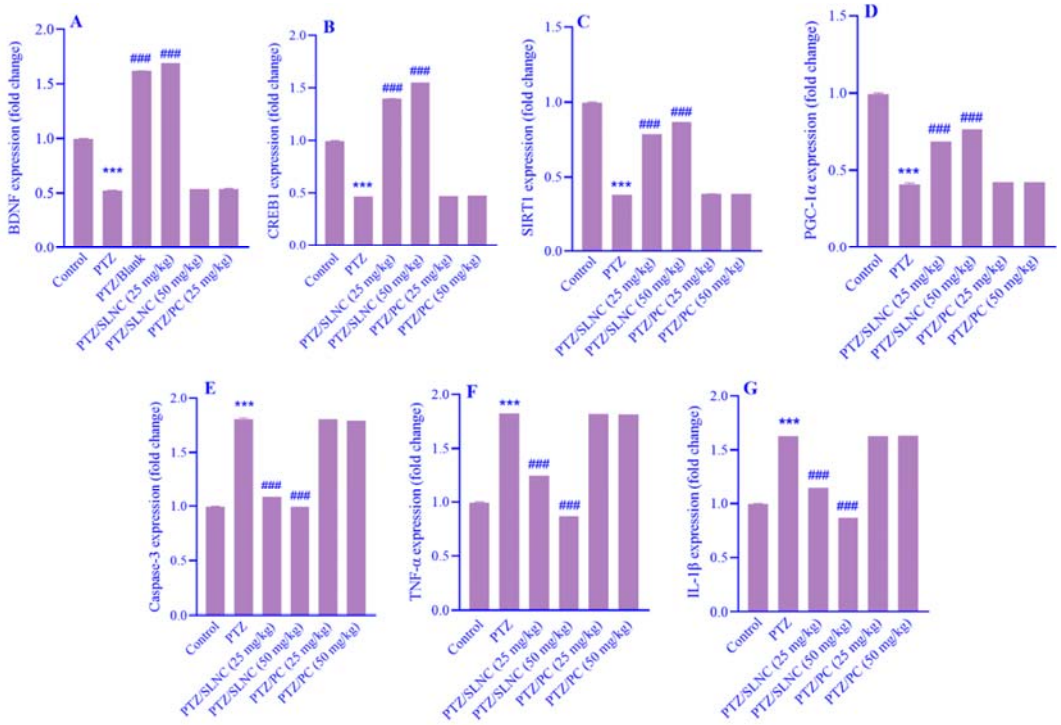

Fig. 8. Effect of the orally administered SLNC and PC on the mRNA expression of (A) BDNF, (B) CREB-1, (C) SIRT1, (D) PGC-1α, (E) caspase-3, (F) TNF-α, and (G) IL-1β in hippocampal tissue of brain in controlled and treated groups. Values are expressed as mean ± SEM. ***$P < 0.001$ indicates significant difference compared to the control group; ###$P < 0.001$ versus the PTZ-treated group. SLNC, Crocin-loaded solid lipid nanoparticle; PTZ, pentylenetetrazol; PC, pure crocin; BDNF, brain-derived neurotrophic factor; CREB, cAMP responsive element binding protein; SIRT1, sirtuin1; PGC-1α, peroxisome proliferator-activated receptor coactivator 1α; TNF-α, tumor necrosis factor-alpha; IL-1β, interleukin-1 beta.

The effect of SLNC and PC treatment on the expression of SIRT1 and PGC-1α

PGC-1α and SIRT1 gene expression, which potentially regulates oxidative damage, significantly reduced in the hippocampal tissue of rats receiving PTZ compared with the control group. Results showed that the expression of these two genes was remarkably enhanced in the hippocampal tissue of rats receiving PTZ plus SLNC (25 and 50 mg/kg) compared with the PTZ group (Fig. 8C and D).

The effect of SLNC and PC treatment on the expression of genes involved in inflammation and apoptosis

In the present study, the anti-apoptotic and anti-inflammatory effects of various doses of SLNC and PC on PTZ-induced epileptic seizures were evaluated through the assessment of mRNA expression of TNF-α, IL-1β, and caspase-3 in the hippocampal tissue. Expression of TNF-α, IL-1β, and caspase-3 significantly increased in the hippocampal tissue of rats receiving PTZ compared to the control group (Fig. 8E-G). The expression of these genes performs a crucial role in the extension of inflammatory hallmarks induced by injections of PTZ. The results showed that the expression of these three genes significantly decreased in the hippocampal tissue of rats receiving PTZ in combination with SLNC (25 and 50 mg/kg) compared with the PTZ group.

Immunohistochemical analysis of SIRT1 expression in the CA1 region of the hippocampus

Figure 9A shows the immunohistochemically staining variations of SIRT1 expression in all rats' hippocampal CA1 and CA3 regions of all groups. In the CA1 and CA3 regions of rats treated with PTZ a significant decrease in SIRT1 area percentage was observed compared to the control group. Likewise, the evaluation of the hippocampal CA1 and CA3 areas of rats receiving PTZ + SLNC (25 and 50 mg/kg) revealed a considerable elevation of SIRT1 percentage compared to the PTZ group, while no meaningful difference between PTZ + PC (25 and 50 mg/kg) compared to the PTZ in CA1 and CA3 regions was observed (Fig. 9B and C).

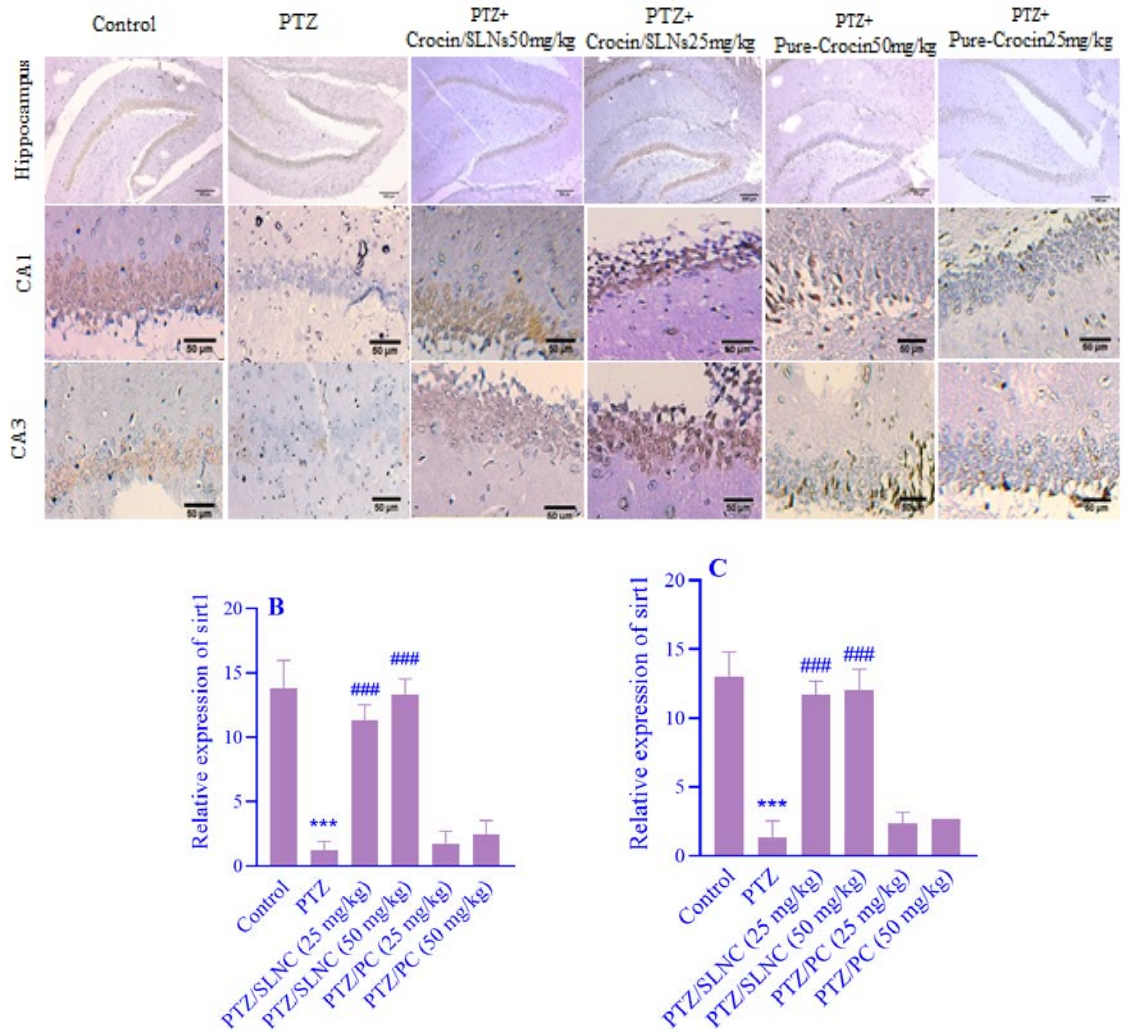

Fig. 9. (A) Representative photomicrograph showing SIRT1 immunohistochemical staining for neurons in hippocampal CA1 and CA3 regions, between different groups. Neurons showed a positive brownish reaction. Scale bars: ~50 µm; (B and C) area percentage for dark neurons SIRT1 in both CA1 and CA3 regions of the hippocampus. Values are expressed as mean ± SEM. ***$P < 0.001$ indicates significant difference compared to the control group; $^{###}P < 0.001$ versus the PTZ-treated group. SLNC, Crocin-loaded solid lipid nanoparticle; PTZ, pentylenetetrazol; PC, pure crocin; SIRT1, sirtuin1.

DISCUSSION

The reaction of brain cells against excessive oxidative stress and the depletion of endogenous antioxidant enzymes eventually leads to cell death and some nervous system disorders, including epilepsy (27-29). Epileptic states may be related to many causes, including mitochondrial impairment and excessive amounts of ROS, which may perform a fundamental role in activating inflammatory cytokines in the brain and progressive memory impairment (30,31). Our study's results showed that after injection of the PTZ-induced seizure model, oxidative stress in brain tissue is potentiated, as determined by elevated MDA levels, formation of ROS, and reduced TAC. The study conducted by Maes *et al*. showed that repetitive seizures are related to high levels of inflammatory biomarkers and oxidative damage, including TNF-a, IL-1B, and MDA (32). In contrast, pretreatment with SLNC decreased seizure-induced neuronal injury in the brain by reducing the formation of MDA

and significantly increasing the TAC production level in the brain tissue compared to the PTZ group. Therefore, antioxidants may protect neurons from seizures. In addition, the beneficial effects of antioxidants have been reported to preserve memory and hippocampal and cortical neurons from seizure-progressive oxidative damage (33). Nevertheless, the results showed the neuroprotective ability of crocin against many neurodegenerative and cognitive impairments. In addition to its pharmacological properties, especially as an antioxidant that scavenges free radicals, crocin has anti-inflammatory and anti-apoptotic effects (34,35). Crocin treatment prevented the decrease in TAC levels and inhibited the increase in MDA. SLNC treatment completely restored TAC and MDA levels in brain tissue. Likely, the prolonged circulation time of crocin is due to another modulatory effect of SLNC. Consistent with the results of the current study, Gokce *et al.* expressed that resveratrol encapsulated with SLN and nanostructured lipid carriers (NLC) decreased the ROS in fibroblast cells (36). The results of this study revealed that PTZ induces a state of neuroinflammation determined by high secretion of inflammatory cytokines (TNF-α and IL-1β) and activation of NF-κB in brain tissue. Neuroinflammation and oxidative damage amplify each other in the temporal promotion of epileptic seizures (37). Excessive ROS production after the seizure begins has been confirmed to activate NF-κB, further increasing the secretion and release of TNF-α and IL-1β (38). Based on our results at mRNA level expression, PTZ injection led to the elevation of the gene expression of TNF-α and IL-1β. Indeed, NF-κB activation leads to an increase in the expression of mRNAs encoding inflammatory cytokines such as IL-1β and TNF-α, which may play a role in seizure-mediated neuronal excitability and neurodegeneration (39,40). Moreover, inhibiting gene expression of TNF-α and IL-1β and reduced levels of TNF-α, IL-1β, and NF-κB in brain tissue mediated by administration of SLNC may attenuate the hippocampal neuronal cell death following PTZ. These results are consistent with those of Jin *et al*. that crocin could suppress the mRNA expression of proinflammatory cytokines (IL-1β, TNF-α, NF-κB, and IL-6) expression (41). Although crocin is a promising platform antioxidant, its principal obstacles are its poor absorption and limited oral bioavailability (42,43). In the current study, SLNC was shown to protect the neuron's cell with antioxidant properties, anti-inflammatory, and anti-apoptotic activities against the PTZ-induced epileptic models in rats. This shows that different doses of SLNC could significantly exert their anti-apoptotic and anti-inflammatory effects on hippocampal tissue. Thus, crocin possessed potent neuroprotective effects promoted by SLNs as a promising carrier system. The prepared SLNC and blank SLNs had good physical and chemical properties. The prepared SLNC has a spherical morphology, a uniform average size of about 98 nm without accumulation, an EE% of 98.33%, and a DL% of 26.8%. The increase in particle size and zeta potential when loading the drug occurs primarily because the drug becomes incorporated into the nanoparticle's structure. This growth also happens due to the interactions between the drug and the nanoparticle's surface and the concentration of the material used in the formulation. The results indicate that the drug's interaction with the functional groups on the nanoparticle's surface, such as hydrogen bonding, can influence the zeta potential. This interaction leads to a higher charge on the nanoparticle's surface, increasing the zeta potential value. Additionally, measuring the zeta potential of the nanoparticles provides valuable information about their storage stability and behavior within the body. Generally, when the zeta potential values are high, the aggregation of nanoparticles decreases. The strong electrostatic repulsion between particles prevents them from clumping together (44,45). Over the past few years, nanocarriers have gained importance for potential drug delivery in the treatment and prevention of central nervous system diseases. The synthesized SLNs having a mean particle size of less than 200 nm make them desirable for prolonged blood circulation, target-specific binding, high stability, and increased permeability of nanoparticles through the BBB, which enhances the likelihood of uptake by the brain (46). A PDI of less than 0.3 represents that the lipid nanoparticles have a uniform size and are in a condition of

monodispersity, with low variation and without aggregation, which is desirable for drug delivery (47). These results of the current showed that the prepared SLNC had uniform particle sizes and spherical shapes. The acquisition of PAL was performed to investigate the cognition-enhancing potential of SLNC. The results showed that PTZ induction impaired memory stabilization and recovery, which may reduce PAL acquisition. Our results indicated that rats with PTZ-induced memory impairment treated with SLNC showed better exploratory ability than those treated with PC, indicating improvement in the PAL acquisition. The neuroprotective effect of crocin can attenuate aversive learning and memory impairment induced by lipopolysaccharide-treated rats (48). Thus, part of the advantageous effects of crocin on cognition function has been related to its brain inhibition of oxidative damage and neuroinflammation (49). Recent research has indicated that increased oxidative damage may perform a key role in the mRNA expression of acetylcholinesterase (AchE), leading to nervous system dysfunction and a gradual decline in cognitive function (50,51). Zhou *et al*. reported that crocin can regulate the levels of Ach and AchE in the region of the cortex and hypothalamus of the AD model, indicating the functioning of the cholinergic system (52). The results also suggest a possible mechanism between the effects of crocin on long-term potentiation in the CA1 area, the inhibitory effect on AChE, and the anti-amyloidogenic activity related to the impact on cognition (53-55). Subsequently, crocin could ameliorate memory and cognitive impairments in mouse models induced by oxidative damage and cerebral hypoperfusion (56,57). In another study, crocin is reported to be weak in improving post-seizure cognitive behavior while significantly reducing the number of recurrent seizures (14). The data of this study indicated that PC may have a weak function in improving cognitive behaviors following injection of PTZ in rats. SLNs are suitable drug delivery systems for enhancing the bioavailability of different phytochemical antioxidants that help alleviate crocin's permeability across the BBB and improve membrane stabilization. However, lipid-based nanocarriers are a key factor in drug-delivery technologies due to their physicochemical properties, including non-toxicity, biocompatibility, success in crossing the body's biological barriers, small size, pharmacokinetic properties, and ability to carry various molecules, transfer of drugs to a target site, and high stability (58,59). The reduction of BDNF expression as an important neurogenic factor for the growth and development of the central nervous system can affect the process of aggravating damage and destruction of nerve tissue (60). Likely enhanced absorption of crocin through SLNC administration may increase the chance of SLNC reaching the brain tissue and crossing the BBB which leads to a better regulatory effect on BDNF and CREB gene expression. As illustrated in Fig. 8A and B, PTZ injection-induced seizures are associated with the downregulation of BDNF and CREB mRNA expression. SLNC administration increased BDNF and CREB mRNA expression in hippocampal tissue more than that of the pure form of crocin. Accordingly, the nuclear transcription factor CREB performs a pivotal role in regulating brain development, neuron survival, the biological function of neuronal cells, and differentiation in the nervous tissue (61). In epileptogenesis, studies have shown that decreasing the activity of the CREB-BDNF pathways is strongly related to the onset of seizures. Based on our outcomes, it has been expressed that the administration of crocin as an antidepressant significantly elevated CREB and BDNF mRNA levels in the hippocampus of rats compared with the saline group. The results of our study were consistent with the research conducted by Vahdati Hassani *et al*. which showed that the administration of crocin as an antidepressant significantly increases CREB and BDNF mRNA levels in the hippocampus of rats compared to the saline group (63). In nervous tissue, SIRT 1 is highly expressed and performs a substantial role in many physiological processes and deacetylation of target proteins such as tumor suppressor p53, PGC-1α, and Forkhead box O1 (1). As PGC-1α is an important regulator in mitochondrial biogenesis, and downregulation of SIRT 1 also reduced PGC-1α expression, it is tempting to identify the obvious relationship between SIRT1/PGC-1α pathways and directly

influence mitochondrial biogenesis that is reasonable for neuron protection in long-lasting seizures (64,65). The effect of epileptogenesis due to increased apoptosis in neurons is caused by the activation of apoptotic proteins such as p53 and caspase-3 (66). Moreover, Chen *et al.* reported that the upregulation of SIRT1 expression inhibits apoptosis-related gene expression, including p53, caspase-3, and Bax (67). The results of the present research demonstrated that PTZ-induced seizure is associated with significantly decreased SIRT 1 and PGC-1α expression, whereas the mRNA level of caspase-3 increased. In addition, we found that SLNC can increase the expression of SIRT1 and PGC-1α and decrease the level of caspase-3 compared with the PTZ group. Besides, SLNC administration appeared to be more effective in activating SIRT1/PGC-1α signaling pathways and inhibiting the apoptosis-associated caspase-3, thereby providing greater protection for the hippocampal neurons in the epilepsy mouse model, when compared to the administration of PC alone. This finding suggests that the SLNC formulation may offer a more favorable therapeutic approach for addressing the neuronal damage associated with epilepsy. Furthermore, the immunohistochemical results in the present study showed that in the CA1 and CA3 regions of rats received SLNC plus PTZ significantly the percentage of SIRT 1 increased compared to the PTZ-treated group. Moreover, there is no meaningful difference between the PC and PTZ groups in CA1 and CA3 regions. A recent report using the schizophrenia model has shown that crocin administration alleviates apoptosis *via* increasing the levels of SIRT 1, nuclear factor erythroid 2-related factor 2, and BDNF in the hippocampus of rats (68). Moreover, our results demonstrated that pretreatment of rats with SLNC upregulates the expression of SIRT 1 in CA1 and CA3 hippocampal areas, suggesting that activation of SIRT 1 by SLNC could be a mechanism that accounts for the neuroprotective effects against PTZ-induced epileptic models in male rats. As given, SLNs are used to improve drug bioavailability, permeability, and absorbability. SLNs are non-toxic, biocompatible, and highly biodegradable small particles. They are lipid-containing, which can be used as a nanocarrier for drugs, making them an excellent option for treating neurological disorders (69,70). Research indicates that SLNs can improve intracellular drug delivery, controlled and sustained release, BBB overcoming, and cerebral bioavailability (71).

CONCLUSION

Given the results of this study, SLNC, a novel formulation strategy, could significantly improve PTZ-induced cognitive decline and oxidative damage. This improvement was attributed to the activation of the SIRT 1/PGC-1α pathway and the decrease in inflammation cytokines. Importantly, the efficacy of crocin was significantly augmented through the utilization of SLNs, as a delivery mechanism. This innovative approach enhanced the bioavailability and targeted delivery of crocin, thereby improving its therapeutic efficacy. Consequently, the combination of crocin and SLNs emerges as a promising treatment option for individuals suffering from epilepsy, offering a potential solution to this debilitating neurological condition.

Conflict of interest statement

The authors declared no conflict of interest in this study.

Acknowledgments

This work, as part of a Ph.D. project, was financially supported by the Research Deputy of Kermanshah University of Medical Sciences through Grant No. 4010117.

Authors' contribution

S. Kakebaraie developed the hypothesis and performed the literature search; S. Kakebaraie, M.R. Gholami, T. Zamir-Nasta, E. Arkan, F. Bahrehmand, and S. Fakhri contributed to the design and conceptualized the experiments described; S. Kakebaraie and C. Jalili analyzed the data and wrote the manuscript; C. Jalili carried out a thorough editing of the text. All authors read and approved the finalized version of the article.

REFERENCES

1. Wang SJ, Zhao XH, Chen W, Bo N, Wang XJ, Chi ZF, *et al*. Sirtuin 1 activation enhances the PGC-1α/mitochondrial antioxidant system pathway in status epilepticus. Mol Med Rep. 2015;11(1):521-526.
   DOI: 10.3892/mmr.2014.2724.
2. Geronzi U, Lotti F, Grosso S. Oxidative stress in epilepsy. Expert Rev Neurother. 2018;18(5): 427-434.
   DOI: 10.1080/14737175.2018.1465410.
3. Anitha A, Thanseem I, Iype M, Thomas SV. Mitochondrial dysfunction in cognitive neurodevelopmental disorders: Cause or effect? Mitochondrion. 2023;69:18-32.
   DOI: 10.1016/j.mito.2023.01.002.
4. Jia X, Wang Q, Ji J, Lu W, Liu Z, Tian H, *et al*. Mitochondrial transplantation ameliorates hippocampal damage following status epilepticus. Animal Model Exp Med. 2023;6(1):41-50.
   DOI: 10.1002/ame2.12310.
5. Li D, Zhang L, Tuo J, Zhang F, Tai Z, Liu X, *et al*. PGC-1α affects epileptic seizures by regulating mitochondrial fusion in epileptic rats. Neurochem Res. 2023;48(5):1361-1369.
   DOI: 10.1007/s11064-022-03834-3.
6. Kupis W, Pałyga J, Tomal E, Niewiadomska E. The role of sirtuins in cellular homeostasis. J Physiol. Biochem. 2016;72(3):371-380.
   DOI: 10.1007/s13105-016-0492-6.
7. Méndez-Armenta M, Nava-Ruíz C, Juárez-Rebollar D, Rodríguez-Martínez E, Gómez PY. Oxidative stress associated with neuronal apoptosis in experimental models of epilepsy. Oxid. Med. Cell. Longev. 2014;2014:293689,1-12.
   DOI: 10.1155/2014/293689.
8. Kamali AN, Zian Z, Bautista JM, Hamedifar H, Hossein-Khannazer N, Hosseinzadeh R, *et al*. The potential role of pro-inflammatory and anti-inflammatory cytokines in epilepsy pathogenesis. Endocr. Metab. Immune. Disord. Drug Targets. 2021;21(10):1760-1774.
   DOI: 10.2174/1871530320999201116200940.
9. Soltani Khaboushan A, Yazdanpanah N, Rezaei N. Neuroinflammation and proinflammatory cytokines in epileptogenesis. Mol. Neurobiol. 2022;59(3): 1724-1743.
   DOI: 10.1007/s12035-022-02725-6.
10. Rashid M, Brim H, Ashktorab H. Saffron, its active components, and their association with DNA and histone modification: a narrative review of current knowledge. Nutrients. 2022;14(16):3317,1-12.
    DOI: 10.3390/nu14163317.
11. Zeinali M, Zirak MR, Rezaee SA, Karimi G, Hosseinzadeh H. Immunoregulatory and anti-inflammatory properties of *Crocus sativus* (Saffron) and its main active constituents: a review. Iran J Basic Med Sci. 2019;22(4):334-344.
    DOI: 10.22038/ijbms.2019.34365.8158.
12. Naderi R, Pardakhty A, Faraji Abbasi M, Ranjbar M, Iranpour M. Preparation and evaluation of crocin loaded in nanoniosomes and their effects on ischemia-reperfusion injuries in rat kidney. Sci Rep. 2021;11(1):23525,1-12.
    DOI: 10.1038/s41598-021-02073-w.
13. Zhong K, Qian C, Lyu R, Wang X, Hu Z, Yu J, *et al*. Anti-epileptic effect of crocin on experimental temporal lobe epilepsy in mice. Front. Pharmacol. 2022;13:757729,1-13.
    DOI: 10.3389/fphar.2022.757729.
14. Hosseinzadeh H, Talebzadeh F. Anticonvulsant evaluation of safranal and crocin from *Crocus sativus* in mice. Fitoterapia. 2005;76(7-8):722-724.
    DOI: 10.1016/j.fitote.2005.07.008.
15. Gupta J, Fatima MT, Islam Z, Khan RH, Uversky VN, Salahuddin P. Nanoparticle formulations in the diagnosis and therapy of Alzheimer's disease. Int J Biol Macromol. 2019;130:515-526.
    DOI: 10.1016/j.ijbiomac.2019.02.156.
16. Mu H, Holm R. Solid lipid nanocarriers in drug delivery: characterization and design. Expert Opin Drug Deliv. 2018;15(8):771-785.
    DOI: 10.1080/17425247.2018.1504018.
17. Scioli Montoto S, Muraca G, Ruiz ME. Solid lipid nanoparticles for drug delivery: pharmacological and biopharmaceutical aspects. Front Mol Biosci. 2020;7:587997,1-24.
    DOI: 10.3389/fmolb.2020.587997.
18. Mukherjee S, Ray S, Thakur RS. Solid lipid nanoparticles: a modern formulation approach in drug delivery system. Indian J Pharm Sci. 2009;71(4):349-358.
    DOI: 10.4103/0250-474X.57282.
19. Yoshino F, Yoshida A, Umigai N, Kubo K, Lee MCI. Crocetin reduces the oxidative stress induced reactive oxygen species in the stroke-prone spontaneously hypertensive rats (SHRSPs) brain. J Clin Biochem Nutr. 2011;49(3):182-187.
    DOI: 10.3164/jcbn.11-01.
20. Yadav A, Sunkaria A, Singhal N, Sandhir R. Resveratrol loaded solid lipid nanoparticles attenuate mitochondrial oxidative stress in vascular dementia by activating Nrf2/HO-1 pathway. Neurochem Int. 2018;112:239-254.
    DOI: 10.1016/j.neuint.2017.08.001.
21. Huang R, Zhu Y, Lin L, Song S, Cheng L, Zhu R. Solid lipid nanoparticles enhanced the neuroprotective role of curcumin against epilepsy through activation of Bcl-2 family and P38 MAPK pathways. ACS Chem. Neurosci. 2020;11(13): 1985-1995.
    DOI: 10.1021/acschemneuro.0c00242.
22. Aghaz F, Vaisi-Raygani A, Khazaei M, Arkan E, Sajadimajd S, Mozafari H, *et al*. Co-encapsulation of tretinoin and resveratrol by solid lipid nanocarrier (SLN) improves mice *in vitro* matured oocyte/ morula-compact stage embryo development. Theriogenology. 2021;171:1-13.
    DOI: 10.1016/j.theriogenology.2021.05.007.

23. Reed LJ. A simple method of estimating fifty percent endpoint. Am J Hyg. 1938;27:493-497. DOI: 10.1093/oxfordjournals.aje.a118408.
24. Jalili C, Salahshoor M, Pourmotabbed A, Moradi S, Roshankhah S, Shabanizadeh Darehdori A, *et al*. The effects of aqueous extract of *Boswellia serrata* on hippocampal region CA1 and learning deficit in kindled rats. Res Pharm Sci. 2014;9(5):351-358. PMID: 25657807.
25. Zamir-Nasta T, Pazhouhi M, Ghanbari A, Abdolmaleki A, Jalili C. Expression of cyclin D1, p21, and estrogen receptor alpha in aflatoxin G1-induced disturbance in testicular tissue of albino mice. Res Pharm Sci. 2021;16(2):182-192. DOI: 10.4103/1735-5362.310525.
26. Cordeiro S, Silva B, Martins AM, Ribeiro HM, Gonçalves L, Marto J. Antioxidant-loaded mucoadhesive nanoparticles for eye drug delivery: a new strategy to reduce oxidative stress. Processes. 2021;9(2):379,1-18. DOI: 10.3390/pr9020379.
27. Espinós C, Galindo MI, García-Gimeno MA, Ibáñez-Cabellos JS, Martínez-Rubio D, Millán JM, *et al*. Oxidative stress, a crossroad between rare diseases and neurodegeneration. Antioxidants (Basel). 2020;9(4):313,1-26. DOI: 10.3390/antiox9040313.
28. Li RJ, Liu Y, Liu HQ, Li J. Ketogenic diets and protective mechanisms in epilepsy, metabolic disorders, cancer, neuronal loss, and muscle and nerve degeneration. J Food Biochem. 2020;44(3):e13140,1-14. DOI: 10.1111/jfbc.13140.
29. Merelli A, Repetto M, Lazarowski A, Auzmendi J. Hypoxia, oxidative stress, and inflammation: three faces of neurodegenerative diseases. J Alzheimers Dis. 2021;82(s1):S109-S126. DOI: 10.3233/JAD-201074.
30. Yuan X, Fu Z, Ji P, Guo L, Al-Ghamdy AO, Alkandiri A, *et al*. Selenium nanoparticles pre-treatment reverse behavioral, oxidative damage, neuronal loss and neurochemical alterations in pentylenetetrazole-induced epileptic seizures in mice. Int J Nanomedicine. 2020;15:6339-6353. DOI: 10.2147/IJN.S259134.
31. Goldberg EM, Coulter DA. Mechanisms of epileptogenesis: a convergence on neural circuit dysfunction. Nat Rev Neurosci. 2013;14(5):337-349. DOI: 10.1038/nrn3482.
32. Maes M, Supasitthumrong T, Limotai C, Michelin AP, Matsumoto AK, de Oliveira Semão L, *et al*. Increased oxidative stress toxicity and lowered antioxidant defenses in temporal lobe epilepsy and mesial temporal sclerosis: associations with psychiatric comorbidities. Mol Neurobiol. 2020;57(8):3334-3348. DOI: 10.1007/s12035-020-01949-8.
33. Ishola IO, Akinleye MO, Afolayan OO, Okonkwo HE, Animashaun OT, Agbaje EO. Anticonvulsant activity of *Nymphaea lotus* Linn. extract in mice: the role of GABAergic-glutamatergic neurotransmission and antioxidant defense mechanisms. Epilepsy Res. 2022;181:106871. DOI: 10.1016/j.eplepsyres.2022.106871.
34. Mohammed El Tabaa M, Mohammed El Tabaa M, Anis A, Mohamed Elgharabawy R, Borai El-Borai N. GLP-1 mediates the neuroprotective action of crocin against cigarette smoking-induced cognitive disorders via suppressing HMGB1-RAGE/TLR4-NF-κB pathway. Int Immunopharmacol. 2022;110:108995,1-13. DOI: 10.1016/j.intimp.2022.108995.
35. Lin L, Liu G, Yang L. Crocin improves cognitive behavior in rats with Alzheimer's disease by regulating endoplasmic reticulum stress and apoptosis. Biomed Res Int. 2019;2019:9454913,1-9. DOI: 10.1155/2019/9454913.
36. Gokce EH, Korkmaz E, Dellera E, Sandri G, Bonferoni MC, Ozer O. Resveratrol-loaded solid lipid nanoparticles versus nanostructured lipid carriers: evaluation of antioxidant potential for dermal applications. Int J Nanomedicine. 2012;7:1841-1850. DOI: 10.2147/IJN.S29710.
37. Terrone G, Balosso S, Pauletti A, Ravizza T, Vezzani A. Inflammation and reactive oxygen species as disease modifiers in epilepsy. Neuropharmacology. 2020;167:107742,1-45. DOI: 10.1016/j.neuropharm.2019.107742.
38. McElroy PB, Liang LP, Day BJ, Patel M. Scavenging reactive oxygen species inhibits status epilepticus-induced neuroinflammation. Exp Neurol. 2017;298(Pt A):13-22. DOI: 10.1016/j.expneurol.2017.08.009.
39. Cheng Y, Wang D, Wang B, Li H, Xiong J, Xu S, *et al*. HMGB1 translocation and release mediate cigarette smoke-induced pulmonary inflammation in mice through a TLR4/MyD88-dependent signaling pathway. Mol Biol Cell. 2017;28(1):201-209. DOI: 10.1091/mbc.E16-02-0126.
40. Zhang S, Hu L, Jiang J, Li H, Wu Q, Ooi K, *et al*. HMGB1/RAGE axis mediates stress-induced RVLM neuroinflammation in mice via impairing mitophagy flux in microglia. J Neuroinflammation. 2020;17(1):15,1-20. DOI: 10.1186/s12974-019-1673-3.
41. Jin W, Zhang Y, Xue Y, Han X, Zhang X, Ma Z, *et al*. Crocin attenuates isoprenaline-induced myocardial fibrosis by targeting TLR4/NF-κB signaling: connecting oxidative stress, inflammation, and apoptosis. Naunyn Schmiedebergs Arch Pharmacol. 2020;393(1):13-23. DOI: 10.1007/s00210-019-01704-4.
42. Zhang Y, Fei F, Zhen L, Zhu X, Wang J, Li S, *et al*. Sensitive analysis and simultaneous assessment of pharmacokinetic properties of crocin and crocetin after oral administration in rats. J Chromatogr B Analyt Technol Biomed Life Sci. 2017;1044-1045:1-7. DOI: 10.1016/j.jchromb.2016.12.003.
43. Lautenschläger M, Sendker J, Hüwel S, Galla HJ, Brandt S, Düfer M, *et al*. Intestinal formation of trans-crocetin from saffron extract (*Crocus sativus L.*) and

in vitro permeation through intestinal and blood brain barrier. Phytomedicine. 2015;22(1):36-44. DOI: 10.1016/j.phymed.2014.10.009.
44. Salatin S, Barar J, Barzegar-Jalali M, Adibkia K, Kiafar F, Jelvehgari M. Development of a nanoprecipitation method for the entrapment of a very water soluble drug into Eudragit RL nanoparticles. Res Pharm Sci. 2017;12(1):1-14. DOI: 10.4103/1735-5362.199041.
45. Kakehbaraei S, Arab-Zozani M, Kakebaraei S. *De novo* hyaluronic acid-based biomaterial: a promising perspective to manage neurodegenerative diseases. Int J Polym Mater Polym Biomater. 2024:1-15. DOI:10.1080/00914037.2024.2360956.
46. Gastaldi L, Battaglia L, Peira E, Chirio D, Muntoni E, Solazzi I, *et al*. Solid lipid nanoparticles as vehicles of drugs to the brain: current state of the art. Eur J Pharm Biopharm. 2014;87(3):433-444. DOI: 10.1016/j.ejpb.2014.05.004.
47. Lippacher A, Müller RH, Mäder K. Preparation of semisolid drug carriers for topical application based on solid lipid nanoparticles. Int J Pharm. 2001;214(1-2):9-12. DOI: 10.1016/s0378-5173(00)00623-2.
48. Azmand MJ, Rajaei Z. Effects of crocin on spatial or aversive learning and memory impairments induced by lipopolysaccharide in rats. Avicenna J Phytomed. 2021;11(1):79-90. PMID: 33628722.
49. Farhadi L, Hojati V, Khaksari M, Vaezi G. Neuroprotective effects of crocin against ethanol neurotoxicity in the animal model of fetal alcohol spectrum disorders. Neurochem Res. 2022;47(4):1001-1011. DOI: 10.1007/s11064-021-03501-z.
50. Lushchekina SV, Kots ED, Novichkova DA, Petrov KA, Masson P. Role of acetylcholinesterase in β-amyloid aggregation studied by accelerated molecular dynamics. BioNanoScience. 2017;7(2):396-402. DOI: 10.1007/s12668-016-0375-x.
51. Zhang JY, Jiang H, Gao W, Wu J, Peng K, Shi YF, *et al*. The JNK/AP1/ATF2 pathway is involved in H_2O_2-induced acetylcholinesterase expression during apoptosis. Cell Mol Life Sci. 2008;65(9):1435-1445. DOI: 10.1007/s00018-008-8047-9.
52. Wang C, Cai X, Hu W, Li Z, Kong F, Chen X, *et al*. Investigation of the neuroprotective effects of crocin *via* antioxidant activities in HT22 cells and in mice with Alzheimer's disease. Int J Mol Med. 2019;43(2):956-966. DOI: 10.3892/ijmm.2018.4032.
53. Geromichalos GD, Lamari FN, Papandreou MA, Trafalis DT, Margarity M, Papageorgiou A, *et al*. Saffron as a source of novel acetylcholinesterase inhibitors: molecular docking and *in vitro* enzymatic studies. J Agric Food Chem. 2012;60(24):6131-6138. DOI: 10.1021/jf300589c.
54. Avgerinos KI, Vrysis C, Chaitidis N, Kolotsiou K, Myserlis PG, Kapogiannis D. Effects of saffron (*Crocus sativus L.*) on cognitive function. a systematic review of RCTs. Neurol Sci. 2020;41(10):2747-2754. DOI: 10.1007/s10072-020-04427-0.
55. Moazen-Zadeh E, Abbasi SH, Safi-Aghdam H, Shahmansouri N, Arjmandi-Beglar A, Hajhosseinn Talasaz A, *et al*. Effects of saffron on cognition, anxiety, and depression in patients undergoing coronary artery bypass grafting: a randomized double-blind placebo-controlled trial. J Altern Complement Med. 2018;24(4):361-368. DOI: 10.1089/acm.2017.0173.
56. Hosseini Dastgerdi H, Radahmadi M, Reisi P. Comparative study of the protective effects of crocin and exercise on long-term potentiation of CA1 in rats under chronic unpredictable stress. Life Sci. 2020;256:118018,1-10. DOI: 10.1016/j.lfs.2020.118018.
57. Soeda S, Aritake K, Urade Y, Sato H, Shoyama Y. Neuroprotective activities of saffron and crocin. Adv Neurobiol. 2016;12:275-292. DOI: 10.1007/978-3-319-28383-8_14.
58. Jalili C, Kiani A, Gholami M, Bahrehmand F, Fakhri S, Kakehbaraei S, *et al*. Brain targeting based nanocarriers loaded with resveratrol in Alzheimer's disease: a review. IET Nanobiotechnol. 2023;17(3):154-170. DOI: 10.1049/nbt2.12127.
59. Gonzalez-Carter D, Liu X, Tockary TA, Dirisala A, Toh K, Anraku Y, *et al*. Targeting nanoparticles to the brain by exploiting the blood-brain barrier impermeability to selectively label the brain endothelium. Proc Natl Acad Sci U S A. 2020;117(32):19141-19150. DOI: 10.1073/pnas.2002016117.
60. Zamir-Nasta T, Abbasi A, Kakebaraie S, Ahmadi A, Pazhouhi M, Jalili C. Aflatoxin G1 exposure altered the expression of BDNF and GFAP, histopathological of brain tissue, and oxidative stress factors in male rats. Res Pharm Sci. 2022;17(6):677-685. DOI: 10.4103/1735-5362.359434.
61. Sharma P, Kumar A, Singh D. Dietary flavonoids interaction with CREB-BDNF pathway: an unconventional approach for comprehensive management of epilepsy. Curr Neuropharmacol. 2019;17(12):1158-1175. DOI: 10.2174/1570159X17666190809165549.
62. Yu X, Guan Q, Wang Y, Shen H, Zhai L, Lu X, *et al*. Anticonvulsant and anti-apoptosis effects of salvianolic acid B on pentylenetetrazole-kindled rats *via* AKT/CREB/BDNF signaling. Epilepsy Res. 2019;154:90-96. DOI: 10.1016/j.eplepsyres.2019.05.007.
63. Vahdati Hassani F, Naseri V, Razavi BM, Mehri S, Abnous K, Hosseinzadeh H. Antidepressant effects of crocin and its effects on transcript and protein levels of CREB, BDNF, and VGF in rat hippocampus. Daru. 2014;22(1):16,1-9. DOI: 10.1186/2008-2231-22-16.
64. Houtkooper RH, Pirinen E, Auwerx J. Sirtuins as regulators of metabolism and healthspan. Nat Rev Mol. Cell Biol. 2012;13(4):225-238. DOI: 10.1038/nrm3293.

65. Chuang YC, Chen SD, Jou SB, Lin TK, Chen SF, Chen NC, *et al*. Sirtuin 1 regulates mitochondrial biogenesis and provides an endogenous neuroprotective mechanism against seizure-induced neuronal cell death in the hippocampus following status epilepticus. Int J Mol Sci. 2019; 20(14):3588.
DOI: 10.3390/ijms20143588.
66. El Nashar EM, Obydah W, Alghamdi MA, Saad S, Yehia A, Maryoud A, *et al*. Effects of *Stevia rebaudiana Bertoni* extracts in the rat model of epilepsy induced by pentylenetetrazol: Sirt-1, at the crossroads between inflammation and apoptosis. J Integr Neurosci. 2022; 21(1):21,1-14.
DOI: 10.31083/j.jin2101021.
67. Chen Y, Xie Y, Wang H, Chen Y. SIRT1 expression and activity are up-regulated in the brain tissue of epileptic patients and rat models. Nan Fang Yi Ke Da Xue Xue Bao. 2013;33(4):528-532.
PMID: 23644113.
68. Sun XJ, Zhao X, Xie JN, Wan H. Crocin alleviates schizophrenia-like symptoms in rats by upregulating silent information regulator-1 and brain derived neurotrophic factor. Compr Psychiatry. 2020;103:152209,1-7.
DOI: 10.1016/j.comppsych.2020.152209.
69. Wei QY, Xu YM, Lau ATY. Recent progress of nanocarrier-based therapy for solid malignancies. Cancers (Basel). 2020;12(10):2783.
DOI: 10.3390/cancers12102783.
70. Khan AR, Yang X, Fu M, Zhai G. Recent progress of drug nanoformulations targeting to brain. J Control Release. 2018;291:37-64.
DOI: 10.1016/j.jconrel.2018.10.004.
71. Graverini G, Piazzini V, Landucci E, Pantano D, Nardiello P, Casamenti F, *et al*. Solid lipid nanoparticles for delivery of andrographolide across the blood-brain barrier: *in vitro* and *in vivo* evaluation. Colloids Surf. Biointerface. 2018;161:302-313.
DOI: 10.1016/j.colsurfb.2017.10.062.